Fast optimization methods for image registration in adaptive radiation therapy

Qiao, Y.

5

Evaluation of an open source registration package for automatic contour propagation in online adaptive intensity-modulated proton therapy of prostate cancer

This chapter was adapted from:

Y. Qiao, T. Jagt, M. Hoogeman, B.P.F. Lelieveldt and M. Staring. **Evaluation of an open source registration package for automatic contour propagation in online adaptive intensity-modulated proton therapy of prostate cancer**, submitted

Abstract

Purpose: To investigate the performance of an open source deformable image registration package, `elastix`, for fast and robust contour propagation in the context of online-adaptive IMPT for prostate cancer.
Material and Methods: A planning and 7-10 repeat CT scans were available of 18 prostate cancer patients. Automatic contour propagation of repeat CT scans was performed using `elastix` and compared with manual delineations in terms of geometric accuracy and runtime. Dosimetric accuracy was quantified by generating IMPT plans using the propagated contours expanded with a 2-mm (prostate) and 3.5-mm margin (seminal vesicles and lymph nodes) and calculating coverage based on the manual delineation. A coverage of $V_{95\%} \geq 98\%$ was considered clinically acceptable.
Results: Contour propagation runtime varied between 13 and 55 seconds for different registration settings. For the fastest setting, 83 in 93 (89.2%), 73 in 93 (78.5%), and 91 in 93 (97.9%) registrations yielded clinically acceptable dosimetric coverage of the prostate, seminal vesicles, and lymph nodes, respectively. For the prostate, seminal vesicles, and lymph nodes the Dice Similarity Coefficient (DSC) $= 0.88 \pm 0.03$, 0.66 ± 0.16, 0.88 ± 0.03 and the mean surface distance (MSD) $= 1.4 \pm 0.3$ mm, 1.8 ± 0.8 mm, 1.5 ± 0.4 mm, respectively.
Conclusions: With a dosimetric success rate of 78.5% to 97.9%, this software may facilitate online adaptive IMPT of prostate cancer using a fast, free and open implementation.

5.1 Introduction

Intensity-modulated proton therapy (IMPT) for prostate cancer treatment has the potential to deliver a highly localized dose distribution to the target volume. However, IMPT is also sensitive to treatment-related uncertainties that may distort the planned dose distribution. These include uncertainties in patient set-up, inter-fraction and intra-fraction variations in the shape and position of the target volume and organs at risk (OARs), and uncertainties in the range of the proton beams [4, 5, 6, 7, 8].

The uncertainties are usually accounted in the clinical-target-volume to planning-target-volume (CTV-to-PTV) margin, while proton-therapy specific effects are accounted for by including robustness in the optimization of the treatment plan. Both come at a price in terms of sparing of OARs. Therefore, ideally, these uncertainties should be tackled at each treatment fraction by re-optimizing the treatment plan, based on a new CT scan-of-the-day. This requires new contours for the target and OARs. Manual re-contouring, however, takes a substantial amount of time, which would give rise to new shape and position uncertainties. Fast automatic methods are therefore mandated.

Deformable image registration (DIR) provides an efficient way to automatically re-contour the repeat CT scan by establishing the spatial correspondence with the planning CT scan. The manual contours from the planning CT are then propagated to the repeat CT, thereby compensating for anatomical changes that may have occurred in the meantime. In combination with fast IMPT treatment replanning this enables the use of small margins and limited amount of robustness without losing dose coverage. The important step of DIR in an online-adaptive IMPT procedure (re-contouring, re-planning, patient-specific QA), however, is currently rather time-consuming. In this chapter we therefore developed and evaluated a fast and automatic DIR method, and performed a dosimetric evaluation for IMPT.

Many DIR algorithms implemented in commercial or open source software packages could be used clinically [104]. Commercial software packages are, however, frequently black boxes for users and have limited choices for parameter customization. Open source packages are much more flexible and provide fully customizable algorithms [105, 106, 10]. Moreover, they support the fundamental scientific principle of reproducibility, sharing of knowledge and thereby promote opportunities for scientific advancement [107, 108, 109].

The validation of DIR for radiation therapy has been performed in terms of dosimetric coverage of the prostate [110, 111, 112] and other anatomical areas [113, 114]. The relation between registration settings and geometric accuracy was also investigated [115]. However, the time cost of image registration [105, 106] is also important for online-adaptive IMPT. Kupelian *et al.* [116] found the prostate having a shift larger than or equal to 5 mm within 30 seconds in 15% of the fractions. Therefore, these shifts should be accounted for by DIR within this time span [117]. In 2009, Godley *et al.* reported 9 minutes to register two CT images [118]. A recent clinical practice report [98] mentioned an average rigid registration time of 79 seconds in their treatment planning, while the computational complexity for DIR was not stated. Another paper presented a matching time of 147 seconds for prostate cancer patients [119], which included the acquisition time and the time for manually matching fiducial markers. Although a graphics processing unit (GPU) and other computational

techniques [106, 22, 120] can be used to accelerate image registration, this has not yet led to real-time and robust algorithms. To our knowledge, the validation of open source packages on registration accuracy in relation to runtime has not been investigated so far for prostate cancer. In this chapter, we investigate the performance of a DIR package, in terms of runtime, geometric and dosimetric performance in IMPT. The presented package, `elastix`, is open source (Apache 2.0 license) and freely available for commercial and clinical application, research and further development.

5.2 Materials and Methods

5.2.1 Patients and imaging

Eighteen patients treated for prostate cancer with IMPT at Haukeland University Hospital in 2007 were included in this study. A planning CT and 7 to 10 repeat CTs were acquired out-of-room for each patient using a Philips Brilliance Big Bore CT scanner and anonymized with DicomWorks version: 2.2.1. Each CT scan contained 90 to 180 slices and were reconstructed with a slice thickness of 2-3 mm. Each slice was of size 512 × 512 pixels and had an in-slice pixel resolution ranging from 0.84 × 0.84 mm to 0.95 × 0.95 mm. Golden fiducial markers (2 to 3) were implanted in the prostate for daily set-up to align the target with the treatment beams [121].

For each CT scan, the prostate, seminal vesicles, lymph nodes, bladder and rectum were delineated by an expert, and independently reviewed by another expert [4]. The original images and delineations are in DICOM-RT format and were converted to meta image format and VTK meshes using MevisLab (`http://www.mevislab.de/`). Manual delineations of the bowels and femoral heads were available for 11 patients, which were included for dosimetric evaluation.

5.2.2 Image registration

In this study, DIR was performed using `elastix` [10] (`http://elastix.isi.uu.nl`). All experiments were performed on a PC with 16 GB memory, Windows 7 operating system and an Intel Xeon E5-1620 CPU with 4 cores (3.6 GHz), utilizing only the CPU, without GPU acceleration.

The planning CT (moving image) was registered to the repeat CT scans (fixed image), after which the manual delineations from the planning CT were propagated based on the DIR results. Registrations were initialized based on the centers of gravity of the bony anatomy (tissue with HU > 200) of the fixed and moving image. A mask of the torso was generated automatically using in-house software Pulmo (commercialized by Medis specials, Leiden, The Netherlands), to eliminate the influence of the couch on image registration quality [50]. The registration procedure includes an affine registration to tackle large movements of organs and is followed by a deformable registration to compensate for local deformations. A fast recursive implementation of B-spline transformation model was used [57, 122]. Mutual information was used as a similarity measure [123]. For optimization we used an accelerated version of adaptive stochastic gradient descent [100]. A three level multi-resolution scheme was chosen to deal with local minima and to reduce calculation burden. Detailed parameter settings are available at the `elastix` website. In the experiments we varied the number of iterations between 100, 500, 1000 and 2000 iterations per resolution, and inspected the influences on DIR quality and runtime.

5.2.3 Evaluation measures

For quantitative evaluation of the automatic DIR method we considered runtime, recontouring quality and dosimetric coverage. Runtime is measured by the system clock, in seconds. The recontouring quality of the prostate, seminal vesicles, lymph nodes, bladder and rectum is measured by comparing the automatically propagated contour from the planning CT with the manual delineation of the repeat CT. We consider the Dice Similarity Coefficient (DSC) [13]:

$$\mathrm{DSC} = \frac{1}{R}\sum \frac{2|\boldsymbol{M} \cap \boldsymbol{F}|}{|\boldsymbol{M}| + |\boldsymbol{F}|}, \tag{5.1}$$

where R is the total number of segmentations, $\boldsymbol{F}$ and $\boldsymbol{M}$ are the manually delineated regions in the fixed image and the propagated regions in the moving image, respectively.

Two types of symmetric surface distances are used, namely the mean surface distance (MSD) and the 95% percentile Hausdorff distance (95%HD). Let $F = \{a_1, a_2, \ldots, a_n\}$, and $M = \{b_1, b_2, \ldots, b_m\}$ represent the mesh points from two surfaces, then we have [124]:

$$\mathrm{MSD} = \frac{1}{2}\left(\frac{1}{n}\sum_{i=1}^{n} d(a_i, \boldsymbol{M}) + \frac{1}{m}\sum_{i=1}^{m} d(b_i, \boldsymbol{F})\right), \tag{5.2}$$

$$\mathrm{HD} = \max\{\max_i\{d(a_i, \boldsymbol{M})\}, \max_j\{d(b_i, \boldsymbol{F})\}\}, \tag{5.3}$$

in which $d(a_i, M) = \min_j \|b_j - a_i\|$. Both distances are computed in 3D. The geometrical success rate γ is defined as the percentage of registrations which have an MSD < 2mm (slice thickness) for the prostate: $\gamma = n\{\mathrm{MSD} < 2\mathrm{mm}\}/N, N = 159$.

To measure the dosimetric impact of differences in manual delineations and automatically delineations, IMPT plans were generated on each repeat CT for both sets of delineations for the 11 patients where delineations of the femoral heads and bowels are available. To evaluate the effect these different delineations have on the dose distributions, both IMPT plans are evaluated on the manual contours, which therefore acts as the ground truth. All IMPT plans were generated using Erasmus-iCycle, an in-house developed treatment planning system [125, 126]. Erasmus-iCycle uses a multi-criteria optimization to generate a clinically desirable Pareto optimal treatment plan on the basis of a wishlist consisting of hard constraints and objectives. A small margin is used (2 mm around the prostate and 3.5 mm around the seminal vesicles and lymph nodes) to compensate for inevitable inaccuracies of the contour-propagation and to account for intra-observer variations in the manual contouring. Note that the margins are far from sufficient to account for shape and positions changes of the target volume, for which clinically typically a margin of 7 mm is used [6, 127, 128]. Dose was prescribed according to a simultaneously integrated boost scheme in which the high-dose PTV (prostate + 2 mm margin) was assigned 74 Gy and the low-dose PTV (seminal vesicles and lymph nodes + 3.5 mm margin) 55 Gy, to be delivered using two laterally opposed beams. The optimization ensures that at least 98% of the target volumes receive at least 95% of the prescribed dose ($V_{95\%} \geq 98\%$). To avoid overdose the optimization ensures that less than 2% of the target volumes receive more than 107% of the highest prescribed dose ($V_{107\%} \leq 2\%$). For the recontouring to be clinically

Table 5.1: Dice overlap of different organs for different registration settings.

	Prostate	Seminal vesicles	Lymph nodes	Rectum	Bladder
Nr. it.	mean ± std	mean ± std	mean ± std	mean ± std	mean ± std
Affine	0.85 ± 0.07	0.47 ± 0.25	0.90 ± 0.04	0.71 ± 0.08	0.78 ± 0.09
100	0.88 ± 0.03	0.66 ± 0.16	0.88 ± 0.03	0.77 ± 0.07	0.88 ± 0.09
500	0.88 ± 0.03	0.68 ± 0.14	0.88 ± 0.03	0.79 ± 0.06	0.89 ± 0.09
1000	0.88 ± 0.04	0.68 ± 0.13	0.87 ± 0.03	0.79 ± 0.06	0.89 ± 0.09
2000	0.87 ± 0.03	0.67 ± 0.13	0.87 ± 0.03	0.80 ± 0.06	0.89 ± 0.10

Table 5.2: Mean surface distance (mm) of different organs for different registration settings.

	Prostate	Seminal vesicles	Lymph nodes	Rectum	Bladder
Nr. it.	mean ± std	mean ± std	mean ± std	mean ± std	mean ± std
Affine	1.64 ± 0.71	2.91 ± 1.65	1.27 ± 0.48	3.92 ± 1.48	4.42 ± 2.10
100	1.36 ± 0.30	1.75 ± 0.84	1.49 ± 0.44	3.16 ± 1.28	2.48 ± 1.77
500	1.40 ± 0.37	1.68 ± 0.79	1.57 ± 0.42	2.97 ± 1.22	2.06 ± 1.46
1000	1.42 ± 0.46	1.67 ± 0.74	1.59 ± 0.42	2.94 ± 1.22	1.99 ± 1.40
2000	1.44 ± 0.50	1.69 ± 0.74	1.61 ± 0.42	2.90 ± 1.20	1.92 ± 1.33

acceptable the automatically generated treatment plans should still fulfill these criteria. The clinical success rate η is defined as the percentage of registrations for which the prostate directly meets the dose treatment criteria: $\eta = n\{V_{95\%} \geq 98\%\}/N$, $N = 93$. A second more conservative measure of clinical success is when all target volumes (the prostate, seminal vesicles and lymph nodes) meet this dosimetric criterium.

5.3 Results

5.3.1 Image registration performance

Examples of automatically propagated contours using DIR are given in Figure 5.1. Table 5.1 presents the overlap after DIR for different number of iterations. For the prostate, we obtained a DSC of 0.88 ± 0.03 for each patient and all settings, and a similar overlap for the lymph nodes. The most difficult structures are the seminal vesicles, which have small volume and only achieved an overlap of 0.66 ± 0.16 for 100 iterations, and 0.67 ± 0.13 for more than 500 iterations. For the OARs, we obtained a DSC of 0.77 ± 0.07 for the rectum and 0.88 ± 0.09 for the bladder for 100 iterations, and small improvements are observed when the number of iterations increased to at least 500. DSC scores generally improved from 100 to 500 iterations, but not after that.

The MSD results are shown in Table 5.2. The MSD of the target organs were smaller than 1.8 mm which was within one voxel ($0.9 \times 0.9 \times 2$ mm). Note that for an increasing number of iterations the MSD slightly increased for the prostate and lymph nodes, likely due to the reduction in MSD of the bladder, rectum and seminal vesicles. The geometrical success rate of the registrations was 96% (153 in 159) for 100 and 500 iterations and 95% (152 in 159) for the other settings, while this value was 77% for affine registration. The 95%HD between the propagated and manual contour is shown in Table 5.3, which shows a similar pattern as the MSD.

Table 5.3: 95% percentile Hausdorff distance (mm) of different organs for different registration settings.

	Prostate	Seminal vesicles	Lymph nodes	Rectum	Bladder
Nr. it.	mean ± std	mean ± std	mean ± std	mean ± std	mean ± std
Affine	3.89 ± 1.67	6.47 ± 3.28	3.12 ± 1.20	11.84 ± 5.70	12.43 ± 6.60
100	3.23 ± 0.98	4.38 ± 2.31	3.66 ± 0.98	10.53 ± 5.75	7.65 ± 6.59
500	3.46 ± 1.44	4.23 ± 2.20	3.93 ± 0.97	10.22 ± 5.82	6.34 ± 5.88
1000	3.51 ± 1.79	4.27 ± 2.26	4.02 ± 0.99	10.27 ± 5.93	6.13 ± 5.63
2000	3.58 ± 1.96	4.38 ± 2.45	4.10 ± 1.03	10.24 ± 5.96	5.93 ± 5.40

The total runtime in seconds for each registration setting was 13.5 ± 1.7, 22.4 ± 1.9, 33.0 ± 2.3, and 54.3 ± 3.1 seconds, for 100, 500, 1000, and 2000 iterations, respectively. Figure 5.2 illustrates the registration accuracy with respect to the mean runtime for different anatomical structures. Boxplots of the Dice overlap, mean surface distance and 95% Hausdorff distance are shown for all registrations ($N = 159$).

5.3.2 Dosimetric validation

All treatment plans were evaluated by visual inspection of the dose distributions, the DVHs of the target volumes and OARs, and the clinical constraints. For the prostate, seminal vesicles and lymph nodes, we report the $V_{95\%}$ and $V_{107\%}$ of each treatment plan that used the DIR-generated contours. For the rectum, we consider V_{45Gy}, V_{60Gy}, V_{75Gy} and D_{mean}, while for the bladder V_{45Gy}, V_{65Gy} and D_{mean} are used, where D_{mean} means the average dose to the structure.

Figure 5.4 shows a boxplot depicting the difference in dosimetric parameters between the automatically generated delineations (100 iterations setting) and the manual delineations, in the treatment plan that was based on the automatically generated delineations. For all dosimetric parameters the median of the differences are close to 0. However, there are some scans for which larger differences occur for especially the $V_{95\%}$ of the seminal vesicles. Table 5.4 shows the percentage of scans for which $V_{95\%} \geq 98\%$ and $V_{107\%} \leq 2\%$ for the treatment plans based on the automatically contoured structures. Note that the success rate when using the manual delineations is close to 100% for all organs. As one can see, DIR using 100 iterations obtained a success rate of 89.2% for the prostate and 78.5% for the seminal vesicles, and these numbers are improved to 89.2% and 88.2%, respectively for 500 iterations. The conservative success rate based on all three target volumes increased from 68.8% to 77.4%, for 100 and 500 iterations, respectively. The 10 out of 93 cases that did not directly meet our definition of clinical success had a $V_{95\%}$ for the prostate between 90% and 97% with a mean of 95% for DIR using 100 iterations. More details are given in the Discussion.

5.4 Discussion

The purpose of this study was to investigate if automatic recontouring for prostate cancer IMPT would be possible, considering the clinical requirements for accuracy, robustness and speed. The overall goal of online adaptive IMPT is to be able to treat with a small margin to spare OARs. This can only be done by daily re-planning,

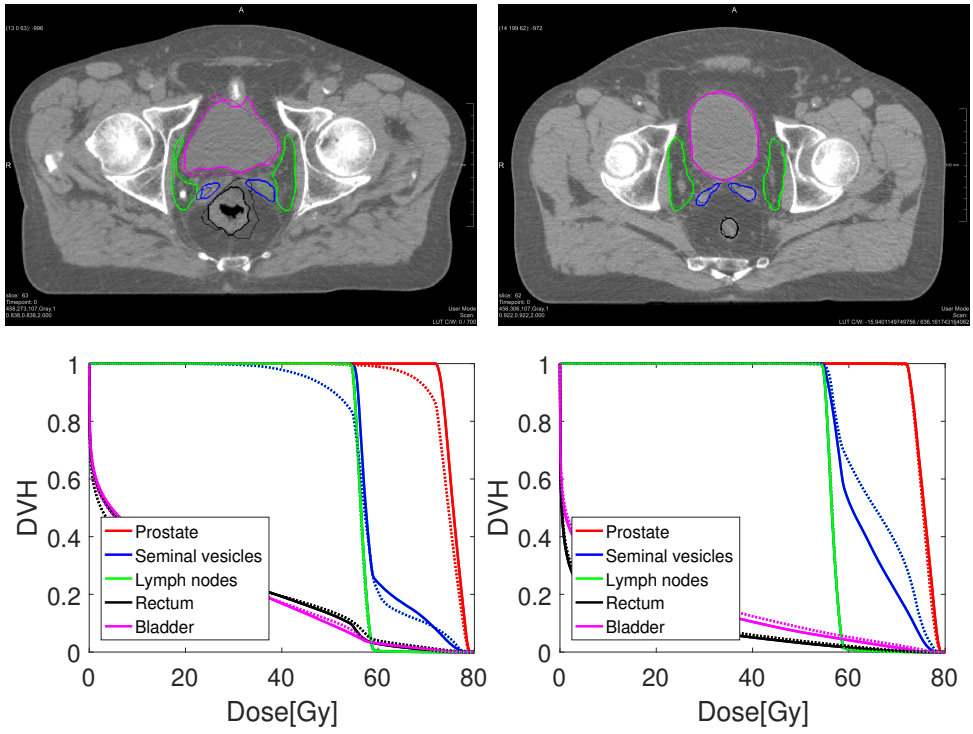

Figure 5.1: An example of one failed case (left) and one successful case (right). The bottom figures are dose volume histograms. The solid line represents the manual contouring results while the dot line is the automatically propagated one with the setting of 100 iterations. For the prostate, the MSD is 2.26 mm and 1.12 mm, while $V_{95\%}$ is 90.80% and 99.83%, respectively. For seminal vesicles, the MSD is 2.74 mm and 1.00 mm, while $V_{95\%}$ is 99.79% and 99.82%, respectively. For lymph nodes, the MSD is 1.45 mm and 0.99 mm, while $V_{95\%}$ both are 100%, respectively.

otherwise coverage loss or underdosage may occur, which is unacceptable. Such daily re-planning warrants automatic recontouring, in this study by DIR. To quantify the clinically more relevant dosimetric impact of such re-planning, we performed a dosimetric validation. The chosen endpoint is therefore $V_{95\%} \geq 98\%$ for each of the target volumes. In general, the registration package `elastix` can automatically re-contour repeat CT scans of the prostate with a desirable accuracy in 13 seconds.

Several aspects were important for registration performance: 1) A correct initialization of DIR was necessary. Alignment of bony anatomy, as used in this study, yielded satisfactory results [4, 129], but exploitation of the implanted gold markers could also be an option [128]; 2) The couch is disturbing the registration and should therefore be removed by masking or cropping. In this study both were used, where cropping was also beneficial for runtime performance; 3) As we had compared the registration accuracy with and without mask, we found that masking is helpful for small volume organs such as the seminal vesicles and rectum, while no differences were observed

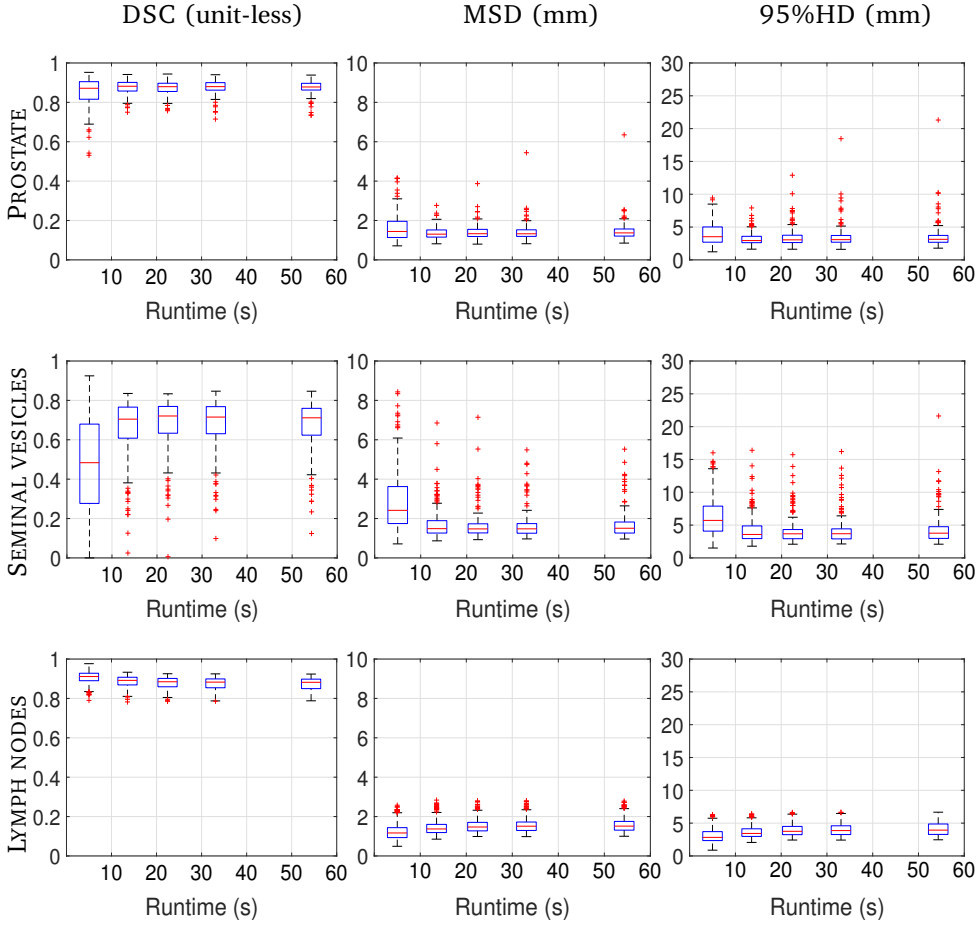

Figure 5.2: Boxplot of registration performance against run time in seconds. From left column to right column the DSC, MSD and 95%HD are shown, respectively. From top to bottom the prostate, seminal vesicles and lymph nodes are shown, respectively. Within one boxplot, from left to right the affine registration and B-spline registrations with 100, 500, 1000 and 2000 iterations are shown, respectively. Each boxplot contains results of 159 registrations.

for the prostate and lymph nodes. This finding is consistent with previous studies [4, 105].

In this study special attention was given to the registration runtime in relation to achieved accuracy, determined by the number of iterations. Overall, registration accuracy increased only slightly when gradually increasing the number of iterations from 100 to 2000, suggesting that early convergence was obtained in most cases. Only for the seminal vesicles an improvement in dose coverage was observed when using 500 iterations, see Table 5.4. The geometrical success rate as expressed by the percentage of registrations with an MSD below the slice thickness of 2 mm was 96%

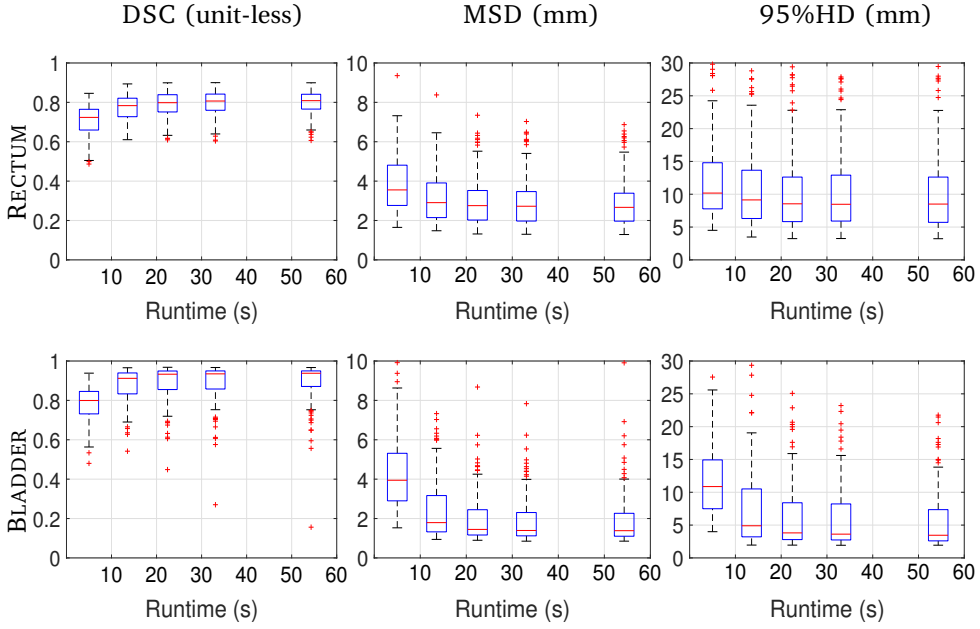

Figure 5.3: Boxplot of registration performance against run time in seconds. From left column to right column the DSC, MSD and 95%HD are shown, respectively. Within one boxplot, from left to right the affine registration and B-spline registrations with 100, 500, 1000 and 2000 iterations are shown, respectively. Each boxplot contains results of 159 registrations.

Table 5.4: Percentage of registrations that meet the dose constraints for the different contours. Conservative success rate (CSR) refers to the percentage of registrations for which all target volumes (the prostate, seminal vesicles and lymph nodes) meet the dose constraints.

		Prostate	Seminal vesicles	Lymph nodes	CSR
$V_{95\%} \geq 98\%$	100	89.2	78.5	97.9	68.8
	500	89.2	88.2	97.9	77.4
	1000	89.2	88.2	98.9	78.5
	2000	90.3	88.2	97.9	77.4
$V_{107\%} \leq 2\%$	100	100.0	100.0	100.0	
	500	100.0	100.0	100.0	
	1000	100.0	100.0	100.0	
	2000	100.0	100.0	100.0	

for the prostate. Clinical success rate, expressed by the dose coverage criteria, was 88% for the prostate. This means that in a high percentage of cases the automatically generated contours can be directly used for online adaptive IMPT. For those patients, smaller margins can be used and less robustness can be included than when using conventional non-adaptive planning, resulting in less dose for the OARs and potentially

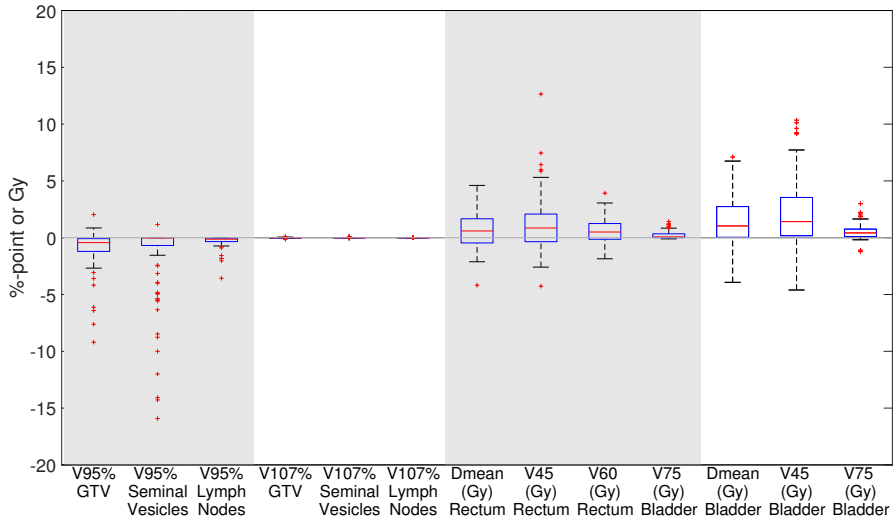

Figure 5.4: Boxplot depicting the difference in dosimetric parameters between the automatically generated delineations and the manual delineations in the treatment plan based on the automatically generated delineations using 100 iterations for 94 scans. Each boxplot indicates the median and the 25^{th} and 75^{th} percentiles of the obtained differences. The line depicts the remaining differences which are not outliers. Values are defined outliers if they are more than 1.5 times the distance between the 25^{th} and 75^{th} quartiles away from the quartiles. The red marks indicate the outliers.

less complications for the patients. For the remaining cases interaction is warranted, for example by manually supplying corresponding points at anatomical regions that require improvement [130, 131].

From the 93 registrations that were assessed in terms of target coverage, 10 (12%) did not directly meet the dose conformity constraints for the prostate. These cases were inspected visually, and we found that 2 cases had many gas pockets in the rectum, while for the other 8 cases no apparent reason was found. For the former we may consider specialized DIR methodology using an intensity modification technique [132]. The MSD of these two cases was around 2.3 mm, and therefore also did not meet the geometrical criteria. Of the 8 remaining cases, one case had a $V_{95\%}$ of 97.99%, which increased to $\geq 98\%$ when 500 or more iterations were used. Two cases had a $V_{95\%}$ around 97% for all settings, which is very close the threshold of 98%; both had an MSD of 1.3 mm, meeting the geometrical criterion for success. Two cases had a $V_{95\%}$ of 96%, which improved to 98% and 99% when 500 iterations or more were used. The remaining three cases obtained a $V_{95\%}$ in the range 92%-96% for the prostate and an MSD in the range 1.6-1.8 mm, so were not far from success.

In order to use `elastix` in a clinical setting, one should consider quality control. This can be done via visual inspection of the generated contours, but assistance by automatic techniques for uncertainty estimation of image registration may be of interest [133, 134]. These techniques may pinpoint areas of possible misregistration,

thus enabling a quicker assessment of registration quality. Secondly, for 12% of cases manual assistance or fall-back strategies are needed. Registration can for example be efficiently improved by manual indicating a few landmarks on structure boundaries [131]. Robustness may be further improved by taking into account automatic estimates of the bladder [135] in the registration by optimizing a joint functional. Thirdly, in this study we used clinical quality repeat CT scan, which assumes the availability of an in-room CT-on-rails system. Since such a system is not available in all hospitals, alternatively Cone Beam CT (CBCT) may be used in-room [114, 136]. However, the reduced soft-tissue contrast of CBCT images may increase the uncertainty of DIR, which therefore may influence the quality of the IMPT plans. Fourthly, the registration time assessed in this chapter is determined by a fixed number of iterations, which is not case-specific [100, 137]. A patient-specific stopping condition for stochastic gradient decent, such as considering a moving average of the noisy cost function values (or gradient), may remedy this. Lastly, a further reduction in runtime may be obtained with the help of a GPU and other computational techniques [106, 22, 120].

5.5 Conclusion

In this study we showed that the open source registration package `elastix` can automatically re-contour repeat CT scans of the prostate in 13 seconds, yielding treatment plans that directly meet the dose conformity constraints in 78.5% to 97.9% of cases, and a geometrical criteria of success in 96% of cases. This software may therefore facilitate online adaptive proton therapy of prostate cancer, enabling a reduction in treatment margins.

Acknowledgement

This study was financially supported by ZonMw, the Netherlands Organization for Health Research and Development [grant number 104003012]; Varian Medical Systems, and the China Scholarship Council [grant number 201206130066]. Erasmus MC Cancer Institute also has research collaborations with Elekta AB, Stockholm, Sweden and Accuray Inc, Sunnyvale, USA. The CT-data with contours were collected at Haukeland University Hospital, Bergen, Norway and were provided to us by responsible oncologist Svein Inge Helle and physicist Liv Bolstad Hysing; they are gratefully acknowledged.